

Glycosaminoglycan-like sulfated polysaccharides from *Vibrio diabolicus* bacterium: Semi-synthesis and characterization

Esposito Fabiana ¹, Vessella Giulia ¹, Sinquin Corinne ², Traboni Serena ¹, Iadonisi Alfonso ¹, Collic-Jouault Sylvia ², Zykwinska Agata ^{2,*}, Bedini Emiliano ^{1,*}

¹ Department of Chemical Sciences, University of Naples Federico II, Complesso Universitario Monte S. Angelo, via Cintia 4, I-80126 Napoli, Italy

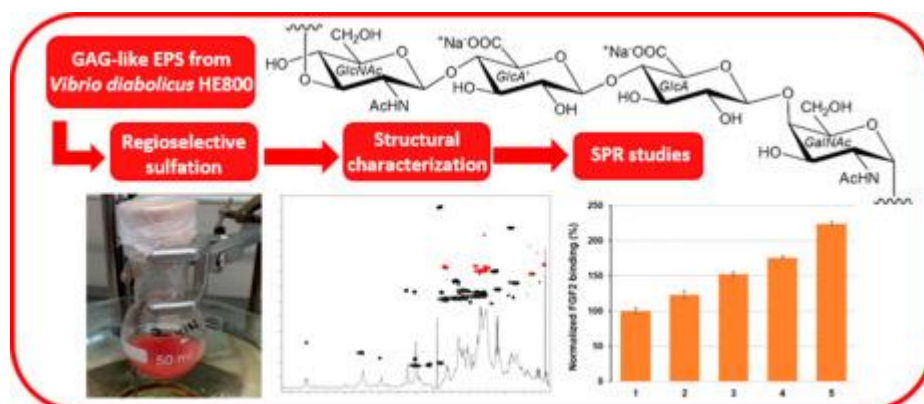
² IFREMER, BRM, 44300 Nantes, France

* Corresponding authors : Agata Zykwinska ; Emiliano Bedini, email address : ebedini@unina.it

Abstract :

Sulfated glycosaminoglycan (GAG) analogues derived from plant, algae or microbial sourced polysaccharides are highly interesting in order to gain bioactivities similar to sulfated GAGs but without risks and concerns derived from their typical animal sources. Since the exopolysaccharide (EPS) produced by the bacterium *Vibrio diabolicus* HE800 strain from deep-sea hydrothermal vents is known to have a GAG-like structure with a linear backbone composed of unsulfated aminosugar and uronic acid monomers, its structural modification through four different semi-synthetic sulfation strategies has been performed. A detailed structural characterization of the six obtained polysaccharides revealed that three different sulfation patterns (per-O-sulfation, a single N-sulfation and a selective primary hydroxylsulfation) were achieved, with molecular weights ranging from 5 to 40 kDa. A Surface Plasmonic Resonance (SPR) investigation of the affinity between such polysaccharides and a set of growth factors revealed that binding strength is primarily depending on polysaccharide sulfation degree.

Graphical abstract



Keywords : Exopolysaccharides, glycosaminoglycans, semi-synthesis, sulfation, growth factors.

1. Introduction

Sulfated polysaccharides are negatively charged biomacromolecules widely distributed in nature. Among them, sulfated glycosaminoglycans (GAGs) play key roles in a plethora of physiological and pathological processes by encoding functional information that modulates extracellular signals such as cell–cell and cell–matrix interactions at tissue and organism levels (Soares da Costa, Reis, & Pashkuleva, 2017). For this reason, some sulfated GAGs, such as heparin,

heparan sulfate and chondroitin sulfate are exploited for therapeutic purposes in pharmaceutical preparations and in food supplements to tackle or prevent several diseases (*e.g.* blood coagulation, articular osteoarthritis, corneal dystrophy) (Köwitsch, Zhou, & Groth, 2018; Restaino et al., 2019). Sulfated GAGs are heteropolysaccharides usually consisting of a linear sequence of variously sulfated disaccharide building blocks, each composed of an aminosugar and a hexose or uronic acid monomer. In dependence of the specific monomeric constituents, four different subclasses of sulfated GAGs can be distinguished: i) heparin and heparan sulfate, ii) chondroitin sulfate, iii) dermatan sulfate, and iv) keratan sulfate (Bedini, Corsaro, Fernández-Mayoralas, & Iadonisi, 2019).

Pharmaceutical- and nutraceutical-grade sulfated GAGs are commonly extracted from animal tissues, even if this raises some problems, such as ethical concerns, the risk of contamination with animal proteins, the difficulty in controlling the distribution of sulfate groups along the polysaccharides (as it depends not only on animal species and tissue but also on the physiopathological conditions – aging, inflammation, tumor formation etc – of the single head of cattle; Collin et al., 2017; Han et al., 2020; Hardingham, 1995). For these reasons in the last two decades researchers put many efforts into opening an access to sulfated GAGs and analogues from non-animal sources (Badri, Williams, Linhardt, & Koffas, 2018; DeAngelis, 2012). Total synthesis of low molecular weight (LMW) species through chemical (Mende et al., 2016) or chemo-enzymatic strategies (Zhang, Lin, Han, & Linhardt, 2020) were reported. Besides, a very promising approach to non-animal sourced sulfated GAGs is based on microbial cell factories, that can be suitably engineered to produce the target polysaccharides themselves (Padi et al., 2021; Jin et al., 2021) or coupled with tailored chemical methods aimed to add sulfate groups at controlled positions of the native, unsulfated polysaccharides from wild-type bacteria (Bedini et al., 2011). Furthermore, by exploiting known or suitably developed new methods for the regioselective insertion of sulfate groups, some research groups obtained sulfated GAG analogues from common polysaccharides (*e.g.* cellulose, chitin, curdlan, alginate) derived from plant, algae or microbial sources (Arlov, Rüttsche, Korayem, Öztürk, & Zerbini-Wong, 2021; Zeng, Groth, & Zhang, 2019). In this frame, a special interest is focused on the sulfation of polysaccharides displaying a GAG-like structure, namely constituted of a linear backbone composed of unsulfated aminosugar and uronic acid or hexose monomers (Lindahl et al., 2005; Vessella et al., 2019). Typical approaches for the controlled sulfation of specific polysaccharide positions rely upon i) direct, regioselective sulfation or desulfation reactions, or ii) multi-step procedures consisting in protecting alcohol moieties at selected positions of the polysaccharide structure, followed by sulfation of the unprotected hydroxyls and then global deprotection (Bedini, Laezza, Parrilli, & Iadonisi, 2017).

The existence of various extreme habitats in marine ecosystem (*e.g.* deep-sea, hydrothermal vents, volcanic and hydrothermal marine areas, marine salterns, sea ice in polar regions) leads to the presence of unusual microorganisms, secreting a plethora of different exopolysaccharides (EPSs) (Casillo, Lanzetta, Parrilli, & Corsaro, 2018). Some of them

show a GAG-like structure (Delbarre-Ladrat, Sinquin, Lebellenger, Zykwinska, & Collicec-Jouault, 2014). In particular, the EPS produced by *V. diabolicus* HE800 strain – a facultatively anaerobic, heterotrophic, mesophilic bacterium, firstly isolated from the polychaete annelid *Alvinella pompejana* collected from a deep-sea hydrothermal field in the East Pacific Rise (Raguénès, Christen, Guezennec, Pignet, & Barbier, 1997) – was shown by 2D NMR spectroscopy to have a tetrasaccharide repeating unit composed of two aminosugars (*N*-acetyl-glucosamine, GlcNAc and *N*-acetyl-galactosamine, GalNAc) and two glucuronic acid (GlcA) units (Figure 1) (Rougeaux, Kervarec, Pichon, & Guezennec, 1999).

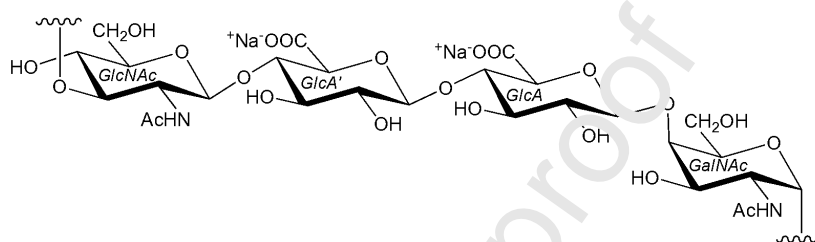


Figure 1: Tetrasaccharide repeating unit of GAG-like HE800 EPS from *V. diabolicus*

EPS from *V. diabolicus* HE800 – named from here below as HE800 EPS – has been already evaluated for its bone regeneration capacity, revealing to act as an efficient filler of bone defects in rat calvaria, without showing any inflammatory activity (Zanchetta, Lagarde, & Guezennec, 2003). Furthermore, a LMW, persulfated derivative of HE800 EPS, obtained through depolymerization of the native polysaccharide followed by a quantitative, non-regioselective sulfation, was shown to exhibit biological activities similar to sulfated GAGs, such as heparin and heparan sulfate (Senni et al., 2013). These promising activities, together with the lack of reports on the selective modification of marine EPSs (Conico, D’Ayala, Malinconico, & Laurienzo, 2008), encouraged an investigation aimed to check the possibility of converting HE800 EPS from a fermentative source into different derivatives carrying sulfate groups at well-defined positions through suitable, regioselective procedures employing tailored sequences of chemical steps (Bedini, Laezza, & Iadonisi, 2016; Palhares et al., 2021). The obtained, semi-synthetic polysaccharides could be characterized from both structural and bioactivity point of view, in order to assess any structure-activity relationship.

2. Materials and methods

2.1. Materials and instruments

Reagents and solvents were used as received from customers, without any further purification. The term “pure water” refers to water purified by a Milli-Q Gradient system (Millipore, Burlington, MA, USA). Dialyses were conducted at 4 °C on Spectra/Por 3.5 kDa cut-off membranes (Repligen, Waltham, MA, USA), except where differently indicated.

Freeze-dryings were performed with a 5Pascal (Trezzano sul Naviglio - MI, Italy) Lio 5P 4K freeze dryer. Centrifugations were performed with an Eppendorf Centrifuge 5804R instrument (Hamburg, Germany) at 4 °C (4600 g, 5 min). A gel filtration chromatography was carried out using an AKTA FPLC system (Cytiva, Marlborough, MA, USA) with refractometric detection (Hitachi L2490, Tokyo, Japan). The column XK 26/100 was filled with 500 mL Superdex 30 preparative grade gel (Cytiva, Marlborough, MA, USA). Ultrafiltration device was composed of a MasterFlex[®] pump (Cole Parmer, Vernon Hills, IL) and a Pellicon holder (Millipore, Burlington, MA, USA). Cassettes of different cut-off (5, 10 or 100 kDa) were mounted for purifications. Molecular mass analyses were performed by a high-performance size-exclusion chromatographic (HP-SEC) system coupled with a multi-angle laser light scattering (MALLS, Dawn Heleos-II, Wyatt Technology, Santa Barbara, CA, USA) and a differential refractive index (RI) (Optilab Wyatt technology, Santa Barbara, CA, USA) detector. HP-SEC system was composed of an HPLC system Prominence (Shimadzu, Kyoto, Japan), a PL aquagel-OH MIXED, 8 µm guard column (7.5 × 50 mm, Agilent Technologies, Santa Clara, CA, USA), and a PL aquagel-OH MIXED separation column (7.5 × 300 mm, Agilent Technologies, Santa Clara, CA, USA). The eluent was aqueous 0.1 M NH₄OAc. Molecular masses were calculated using a refractive index increment characteristic of polysaccharide, $dn/dc = 0.145 \text{ mL/g}$. Monosaccharide composition of the native HE800 EPS and the LWM HE800 EPS was determined according to Kamerling *et al.* (1975) method, modified by Montreuil *et al.* (1986). Briefly, samples were hydrolyzed using HCl/MeOH at 100 °C for 4 h. Myo-inositol was used as internal standard. The methyl glycosides thus obtained were then converted to their trimethylsilyl derivatives using a 99:1 v/v *N,O*-bis(trimethylsilyl)trifluoroacetamide - trimethylchlorosilane (BSTFA:TMCS) mixture. Gas-chromatography (GC-FID, Agilent Technologies 6890N) was used for separation and quantification of the obtained per-*O*-trimethylsilyl methyl glycosides.

2.2. NMR spectra acquisition

NMR spectra were recorded on a Bruker Avance III (¹H: 600 MHz, ¹³C: 150 MHz) or on a Bruker Avance III HD (¹H: 400 MHz, ¹³C: 100 MHz) instrument (Billerica, MA, USA) – the former equipped with a cryo-probe – in D₂O (acetone as internal standard, ¹H: (CH₃)₂CO at δ 2.22 ppm; ¹³C:(CH₃)₂CO at δ 31.5 ppm). Bruker TopSpin 4.0.5 software was used for all the experiments. Gradient-selected COSY and TOCSY experiments were performed using spectral widths of either 6000 Hz in both dimensions, using data sets of 2048 × 256 points. TOCSY mixing time was set to 120 ms. ¹H,¹³C-DEPT-HSQC experiments were measured in the ¹H-detected mode via single quantum coherence with proton decoupling in the ¹³C domain, using data sets of 2048 × 256 points and typically 100 increments. As for ¹H,¹³C-HSQC-TOCSY and ¹H,¹³C-HMBC, data sets of 2048 × 256 points were used, with 120 increments, and the mixing time for ¹H,¹³C-HSQC-TOCSY was set to 120 ms.

2.3. Binding studies with growth factors

Surface Plasmonic Resonance (SPR) experiments were carried out on a Biacore T200 instrument (Cytiva, Washington, DC, USA). Transforming Growth Factor- β 1 (TGF- β 1), Bone Morphogenetic Protein-2 (BMP-2), Vascular Endothelial Growth Factor (VEGF), Growth Differentiation Factor-5 (GDF-5), Fibroblast Growth Factor-2 (FGF-2) and Epidermal Growth Factor (EGF) were covalently immobilized to the dextran matrix of a CM5 sensor chip (Cytiva, Washington, DC, USA), as recommended by the manufacturer at a flow rate of 5 μ L/min. Binding assays of the different HE800 derivatives and heparin (15,000 g/mol, H4784 Sigma), used as reference, were performed in 10 mM HEPES at pH 7.4 containing 150 mM NaCl and 0.005% P20 surfactant (HBS-P buffer, Cytiva, Washington, DC, USA) with dissociation monitored for 15 min. Regeneration was achieved with NaOH (4.5 mM/L) after each cycle. The resulting sensorgrams were fitted using BiaEval T200 (Cytiva, Washington, DC, USA).

2.4. Production of the native HE800 EPS.

Native HE800 EPS was prepared according to previous reports (Ragu  s, Christen, Guezennec, Pignet, & Barbier, 1997; Rougeaux, Kervarec, Pichon, & Guezennec, 1999). Briefly, *V. fischeri* HE800 was cultured at 25 $^{\circ}$ C in Marine Broth 2216 medium at pH 7.2 in a 2L fermenter. Glucose at 30 g/L was added as a carbon source. After 48 h of fermentation, the culture medium was centrifuged at 9000 g for 5 min, the supernatant containing soluble EPS was ultrafiltrated on a 100 kDa cut-off membrane and freeze-dried.

2.5. LMW HE800 EPS.

LMW HE800 EPS was prepared, as previously described (Senni et al., 2013). Briefly, the native EPS (2.5 g) solubilized in pure water (350 mL) was depolymerized at 60 $^{\circ}$ C for 45 min using H₂O₂ added dropwise (530 μ L at 30%) in the presence of copper (II) acetate (Cu(OAc)₂, 18 mg), used as catalyst. After overnight reduction by sodium borohydride (NaBH₄) at rt and purification on Chelex[®] 20 resin, the solution containing depolymerized EPS was ultra-filtrated on a 5 kDa cut-off membrane and freeze-dried. To obtain a homogeneous fraction with low polydispersity, a predominant population of the polysaccharide chains was selected by a gel filtration chromatography on Superdex[®] 30, using an AKTA FPLC system coupled with a refractometric detector. Samples eluted with pure water were pooled and freeze-dried.

2.6. Polysaccharide 2

LMW HE800 EPS (33.9 mg, 34.4 μ mol repeating unit) was dissolved in pure water (750 μ L) and passed through a short Dowex 50 WX8 column (H⁺ form, 20-50 mesh, approx. 4 cm³). Elution with deionized water was continued until a neutral pH of the eluate was detected. The eluted fraction was then neutralized with some drops of an aqueous solution of tetra-*n*-butylammonium hydroxide (TBAOH; 16% w/v TBAOH in H₂O). After freeze-drying, polysaccharide **1** (43.8 mg, 129% mass yield) was obtained as a white waxy solid. A suspension of **1** (41.2 mg, 33.2 μ mol repeating unit) in dry *N,N*-dimethylformamide (DMF, 2.5 mL) was then treated with a 0.40 M solution of

pyridine-sulfur trioxide complex ($\text{SO}_3\cdot\text{py}$) in dry DMF (550 μL , 199 μmol). After 1 h stirring at 4 $^\circ\text{C}$, some drops of aqueous 1 M NaHCO_3 were added to adjust pH to 7 and then aqueous 0.3 M NaCl (5 mL) was added. The mixture was stirred for 1 h at rt, then dialyzed and freeze-dried. The obtained product was dissolved in pure water and passed through a short Dowex 50 WX8 column (H^+ form, 20-50 mesh, approx. 4 cm^3), continuing the elution with pure water until a neutral pH of the eluate was detected. The eluted solution was adjusted to pH 10 with aqueous 1 M NaOH , then dialyzed and freeze-dried to afford polysaccharide **2** (15.9 mg, 39% mass yield) as a white solid.

2.7. Polysaccharide 4.

Highly sulfated LMW HE800 EPS (polysaccharide **4**) was obtained by direct sulfation of LMW HE800 EPS, as described earlier (Senni et al., 2013). Briefly, LMW HE800 EPS (50.0 mg, 50.5 μmol repeating unit) was dissolved in pure water (5 mL) and passed through a Dowex 50 WX8 column (H^+ form, 20-50 mesh, approx. 8 cm^3). After elution with pure water, the fraction was neutralized with pyridine added dropwise. After freeze-drying, LMW HE800 EPS pyridinium salt **3** was firstly solubilized in dry DMF (25 mL) at 45 $^\circ\text{C}$ for 2 h under continuous stirring and then sulfated for the next 2 h at 45 $^\circ\text{C}$ in the presence of $\text{SO}_3\cdot\text{py}$ (250 μg , 1.57 mmol). Some drops of aqueous 3 M NaOH were then added to adjust pH to 7. The mixture was then dialyzed against pure water for three days prior to be freeze-dried to afford polysaccharide **4** (101.8 mg, 204% mass overall yield) as a white solid.

2.8. Polysaccharide 5

Per-*O*-sulfated polysaccharide **4** (18.8 mg, 9.12 μmol repeating unit) was dissolved in pure water (1.0 mL) and passed through a short Dowex-50 WX8 column (H^+ form, 20–50 mesh, approx. 4 cm^3). Elution with pure water was continued until pH of the eluate was neutral. The obtained eluate was treated with some drops of pyridine to neutralize the solution. Freeze-drying of the collected eluate gave per-*O*-sulfated LMW HE800 EPS pyridinium salt, that was in turn suspended in pyridine (1.7 mL) and treated with *N*-methyl-*N*-(trimethylsilyl)-trifluoroacetamide (MTSTFA, 31 μL , 0.16 mmol) for a 6-*O*-desulfation in order to convert the released hydroxyl groups into trimethylsilyl ethers. After 20 h stirring at 70 $^\circ\text{C}$, the mixture was cooled to rt, then pure water (3 mL) was added giving a turbid mixture that was dialyzed for one day. Thereafter, the mixture was passed through a short Dowex-50 WX8 column (H^+ form, 20–50 mesh, approx. 4 cm^3), continuing the elution with pure water until a neutral pH of the eluate was reached. Then some drops of aqueous 1 M NaOH were added to neutralize the solution. Dialysis and subsequent freeze-drying gave polysaccharide **5** (12.2 mg, 65% mass overall yield) as a white solid.

2.9. Polysaccharide 6

LMW HE800 EPS (40.5 mg, 50.5 μmol repeating unit) was dissolved in hydrazine monohydrate ($\text{N}_2\text{H}_4\cdot\text{H}_2\text{O}$, 64-65% hydrazine in water, 1.0 mL), then hydrazine sulfate salt ($\text{N}_2\text{H}_4\cdot\text{H}_2\text{SO}_4$, 10.0 mg, 76.8 μmol) was added. The suspension was flushed under Ar atmosphere and heated at 90 $^\circ\text{C}$. At different times (10, 20, 30 and 40 hours), 250 μL aliquots

were collected, cooled to rt and treated with ethanol (1.0 mL) and a few drops of brine. The mixtures were dialyzed and freeze-dried. The sample obtained from a 20 hours *N*-deacetylation reaction was named as **6** and employed for further reaction to polysaccharide **7**.

2.10. Polysaccharide **7**

Polysaccharide **6** (15.6 mg, 19.3 μmol repeating unit) was dissolved in pure water (3.9 mL) and treated with Na_2CO_3 (25.0 mg, 23.6 μmol) and trimethylamine-sulfur trioxide complex ($\text{SO}_3\cdot\text{Me}_3\text{N}$, 25.0 mg, 18.0 μmol) and heated at 45 $^\circ\text{C}$. After 4 h stirring, a second aliquot of $\text{SO}_3\cdot\text{Me}_3\text{N}$ (25.0 mg, 18.0 μmol) was added to the solution. After 20 h stirring at 45 $^\circ\text{C}$, the obtained solution was cooled to rt, dialyzed and freeze-dried to yield polysaccharide **7** (12.4 mg, 79% mass yield) as a white solid.

2.11. Polysaccharide **8**

LMW HE800 EPS (20.8 mg, 25.9 μmol repeating unit) was suspended in dry DMF (1.0 mL) and then heated to 80 $^\circ\text{C}$. After 1 h stirring, a very fine suspension was obtained. It was cooled to rt and treated with α,α -dimethoxytoluene (39 μL , 259 μmol) and then with (+)-camphor-10-sulfonic acid (CSA, 1.5 mg, 6.5 μmol). The mixture was stirred for 20 h at 80 $^\circ\text{C}$. Thereafter, it was cooled to rt and treated with diisopropyl ether (5 mL). The obtained white precipitate was collected by centrifugation and then dried under vacuum to afford derivative **8** (24.8 mg, 119% weight yield) as a white solid.

2.12. Polysaccharide **9**

A suspension of polysaccharide **8** (17.8 mg, 20.3 μmol repeating unit) in dry DMF (500 μL) was treated with a 0.4 M solution of $\text{SO}_3\cdot\text{py}$ in dry DMF (2.7 mL, 1.1 mmol). After overnight stirring at 50 $^\circ\text{C}$, the obtained clear solution was cooled to rt and then a saturated NaCl solution in acetone (5 mL) was added. The obtained white precipitate was collected by centrifugation and then dissolved in pure water (1 mL). The acid solution (pH \sim 2) was heated to 50 $^\circ\text{C}$ and stirred for 2.5 hours. Thereafter, it was treated at rt with an aqueous 4 M NaOH solution to adjust pH to 12. The solution was stirred at rt for 20 h and then neutralized with aqueous 1 M HCl. Dialysis and freeze-drying yielded polysaccharide **9** (31.5 mg, 177% weight yield) as a white solid.

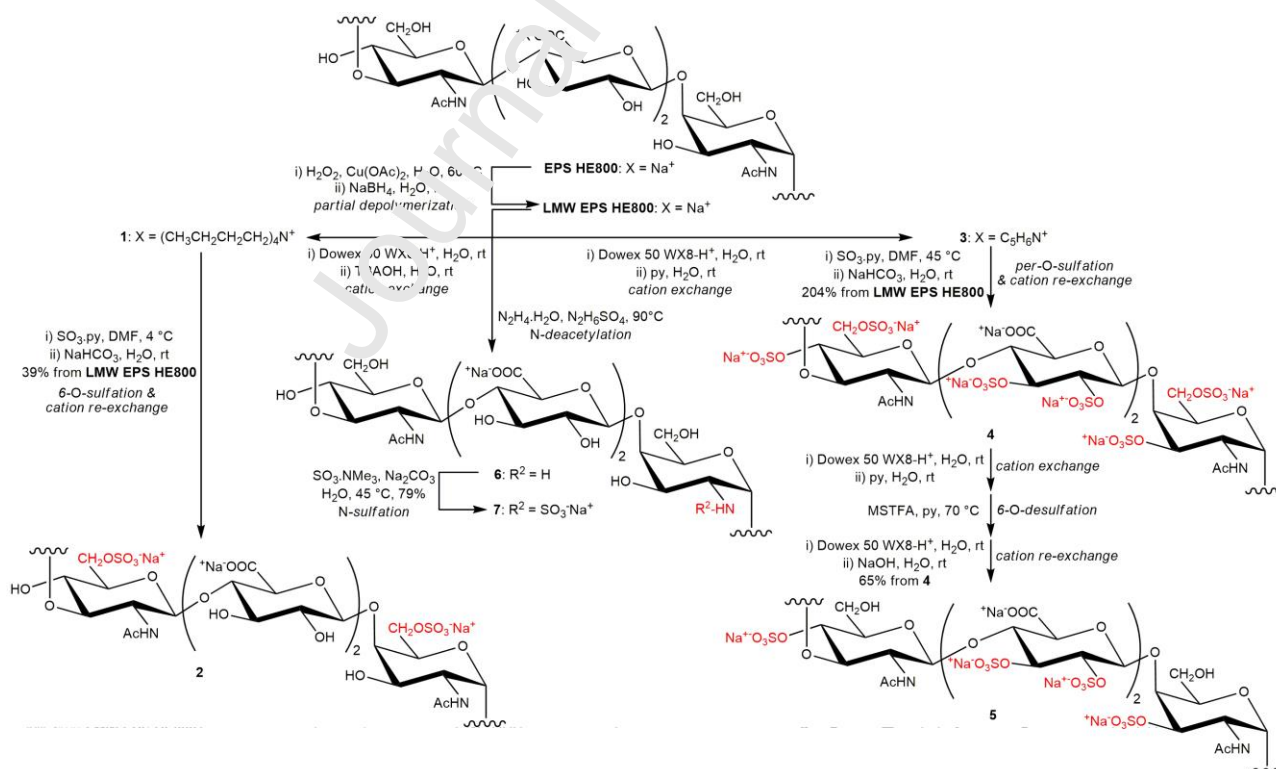
3. Results and Discussion

3.1 Semi-synthesis of GAG-like sulfated polysaccharides from LMW HE800 EPS

Sulfated polysaccharides employed for some applications can cause in some cases adverse effects, that are associated with high molecular weight sulfated species (Fonseca et al., 2010; Lin et al. 2021), Therefore, HE800 EPS produced by *V. diabolicus* HE800 fermentation under controlled conditions, was partially depolymerized through a H_2O_2 -mediated free radical reaction to give a LMW HE800 EPS (approx. 24 kDa, Table 1) before any sulfate group insertion. A

constant GlcNAc/GlcA/GalNAc molar ratio of 1/2/1, determined by monosaccharide composition analysis of the native HE800 EPS and the LMW HE800 EPS, demonstrated that the depolymerization process had no major impact on the polysaccharide structure.

A direct, regioselective sulfation under mild conditions (Valoti, Miraglia, Bianchi, Valetti, & Bazza, 2012) of the most reactive, primary alcohol moieties of GlcNAc and GalNAc was firstly attempted. To this aim, a cation exchange step converted LMW HE800 EPS into its tetrabutylammonium salt **1**, that was then solubilized in DMF and treated with $\text{SO}_3 \cdot \text{py}$ at 4 °C. Finally, a cation re-exchange step could afford sulfated polysaccharide sodium salt **2**, presumably having sulfate groups exclusively placed at position O-6 of GlcNAc and GalNAc units (Scheme 1). The obtaining of a complementary sulfation pattern, with every alcohol moiety sulfated excepting the primary hydroxyls at GlcNAc and GalNAc C-6 sites, was attempted through a selective desulfation reaction on the per-O-sulfated HE800 EPS derivative **4**, that was obtained in turn by sulfation of LMW EPS HE800 pyridinium salt **3** with $\text{SO}_3 \cdot \text{py}$ in DMF at 45 °C. The following desulfation reaction was performed on the pyridinium salt of **4** with MTSTFA, a reagent known to cleave sulfate groups selectively placed at primary positions of polysaccharides and to convert the released hydroxyl groups into trimethylsilyl ethers, that can be then easily cleaved by an aqueous work-up (Takano, R., Kanda, T., Hayashi, K., Yoshida, K., & Hara, 1995). Therefore, the structure reported in Scheme 1 could be tentatively assigned to the obtained polysaccharide **5**.



Scheme 1: Direct strategies for selective sulfation of LMW HE800 EPS

(mass yields are reported; expected structures are depicted; see text and Table 1 for structural characterization of derivatives 2-7)

A third, direct strategy for the selective sulfation of LMW HE800 EPS aimed to substitute the acetamido moieties of GlcNAc and GalNAc units with *N*-linked sulfate groups. To this aim, the *N*-acetyl groups should firstly be cleaved under appropriate conditions, then the liberated amino functions should chemoselectively be sulfated. Hydrazinolysis is the typically employed reaction for GAG *N*-deacetylation (Nadkarni et al., 1996). Reaction parameters, such as temperature, catalyst, hydrazine content and reaction time, play a pivotal role in determining its efficiency and avoiding side-reactions (Guo & Conrad, 1989; Zhao et al., 2013). Indeed, GAG structures are quite labile under the required alkaline condition, that could cause a β -eliminative cleavage at the glycosidic bonds involving *O*-4 linked uronic units, thus resulting in an undesired depolymerization. Since HE800 EPS structure displays *O*-4 linked GlcA units as well, a reaction optimization was judged necessary. In particular, since reaction temperature (not higher than 90 °C) and hydrazine content (not higher than 70% in water) parameters are already well established (Yan et al., 2017; Zhao et al., 2013) as well as the use of hydrazine sulfate salt as catalyst to accelerate the *N*-deacetylation reaction, we focused exclusively on reaction time for the optimization study. Thus, the reaction was conducted with $\text{N}_2\text{H}_4\cdot\text{H}_2\text{O}$ and $\text{N}_2\text{H}_4\cdot\text{H}_2\text{SO}_4$ at 90 °C for different times (10, 20, 30 and 40 hours). A comparison of ^1H -NMR spectra of starting LMW HE800 EPS and of the obtained derivatives (Figure 2) clearly showed a lowering of the intensity of the α -linked GalNAc *H*-1 signal at δ 5.42 ppm with the reaction time, together with the concomitant appearance of a new resonance at δ 5.67 ppm, which could be attributed to the anomeric proton of the *N*-deacetylated GalN units. However, at reaction times higher than 20 hours (Figure 2-d,e) overlapped peaks could be observed in the range 5.62–5.72 ppm, reasonably due to anomeric signals of GalN units in shorter and/or differently degraded polysaccharide chains. Surprisingly, even in the case of a 40 hours reaction (Figure 2-e), the region of the spectrum in the range 1.90-2.10 ppm – typically associated to acetyl CH_3 resonances – displayed residual, not negligible signals. A detailed 2D-NMR analysis of the polysaccharide derivative obtained after 20 hours reaction was conducted in order to characterize it in full details. Its $^1\text{H},^{13}\text{C}$ -DEPT-HSQC spectrum displayed four anomeric signals ($\delta_{\text{H,C}}$ 5.67/97.2, 4.72/104.2, 4.60/101.5 and 4.52/103.9 ppm; Supporting Information), that could be assigned to GalN, GlcA, GlcNAc and GlcA' residues, respectively, by the aid of COSY and TOCSY 2D-NMR spectra. This revealed that the *CH*-1 signal of glucosamine residues underwent no significant ^1H and ^{13}C shifts with respect to starting LMW-HE800 EPS values (Figure 2 and Supporting Information). Similarly, the *CH*-2 resonance of the glucosamine units remained unaffected after the *N*-deacetylation reaction, while its galactosamine counterpart was significantly upfield shifted in the ^1H dimension (from 4.27 to 3.68 ppm) and slightly downfield shifted in the ^{13}C one (from 51.3 to 52.4 ppm). The observed NMR shifts, in agreement with reported data on

N-deacetylation of GAGs (Li et al., 2014; Mans et al., 2015), suggested that the *N*-deacetylation reaction involved exclusively GalNAc units, leaving unaltered the GlcNAc residues. The latter could not be deacetylated even under prolonged reaction times. Presumably, the acetamido moiety of GalNAc units is more labile to hydrazinolysis with respect to GlcNAc one, and the formation during the course of the reaction of an ammonium cation on GalN units hinders the development of a further positive charge on the adjacent GlcN sites.

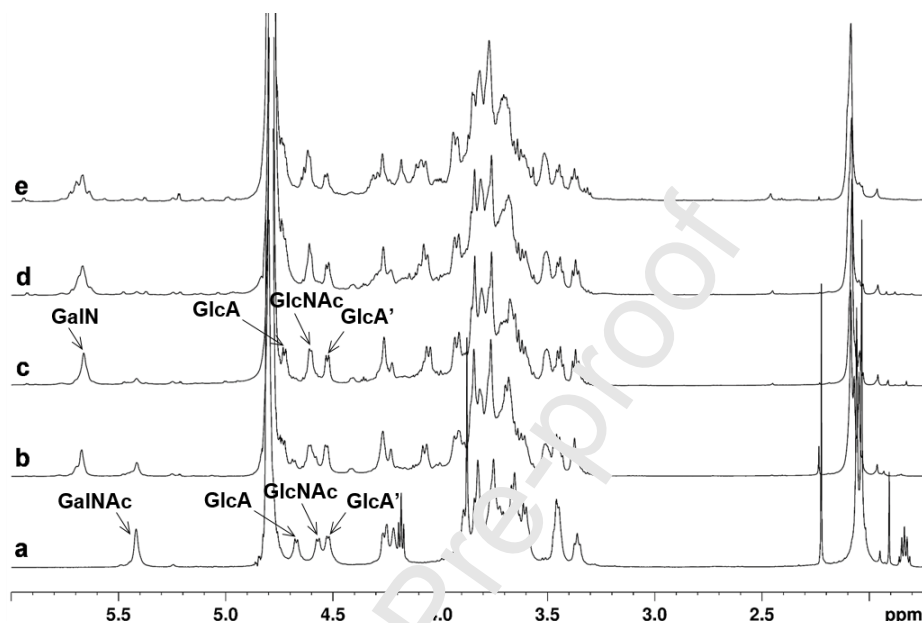
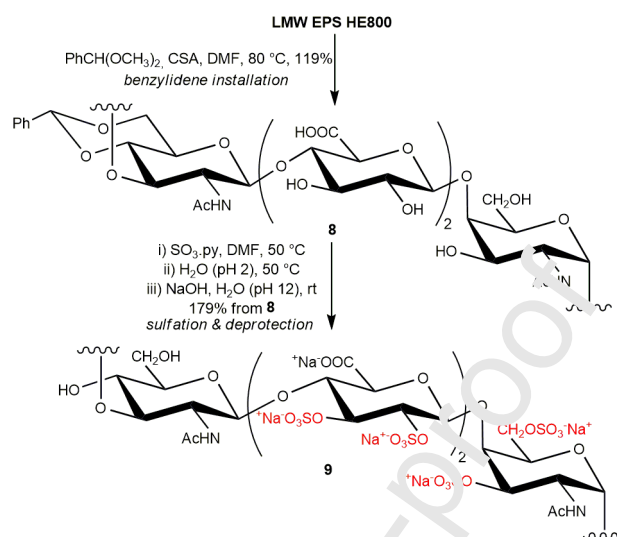


Figure 2: ¹H NMR spectra (zoom, 600 MHz, 298 K, D₂O) of (a) LMW-HE800 EPS and (b-e) derivative **6** obtained after 10, 20, 30 or 40 hours, respectively, under hydrazinolysis reaction (only anomeric signals assignment is displayed)

Derivative **6**, obtained under the hydrazinolysis conditions indicated above after 20 hours reaction, was subjected in turn to a chemoselective sulfation of the single free amine with SO₃·Me₃N. This sulfating agent was selected due to its lower reactivity with respect to other commonly employed ones (*e.g.* SO₃·py, SO₃·DMF). This can be ascribed to the higher Lewis base strength of trimethylamine. *N*-sulfation was conducted in water at 45 °C in the presence of Na₂CO₃ (Li et al., 2014).

In addition to direct, regioselective sulfation or desulfation reactions, a multi-step procedure was also attempted on LMW HE800 EPS in order to gain an additional derivative with an alternative sulfation pattern. This fourth strategy was based upon the contemporary protection of two alcohol moieties with an acetal-type cyclic protecting group (CPG), followed by sulfation and deprotection. Although widely used in synthetic mono- and oligosaccharide chemistry, in the case of polysaccharides CPGs employment has been reported only in few, scattered examples (Bachelder, Pino, & Ainslie, 2017; Chien, Enomoto, & Iwata, 2019; Laezza, De Castro, Parrilli, & Bedini, 2014; Sakamoto et al., 2017). Here a benzylidene acetal-type CPG was selected for the exclusive protection of 1,3-diol at 4 and 6 position of GlcNAc units of LMW HE800 EPS. The reaction was conducted with α,α -dimethoxytoluene in the presence of (+)-camphor-10-

sulfonic acid (CSA) as acid catalyst (Vessella et al., 2021) to give derivative **8**, that was subjected in turn to per-*O*-sulfation with $\text{SO}_3\cdot\text{py}$ in DMF at 50 °C followed by benzylidene deprotection through an acid-catalyzed hydrolysis (Scheme 2).



Scheme 2: Multi-step strategy for selective sulfation of LMW HE800 EPS

(mass yields are reported; expected structures are depicted; see text and Table 1 for structural characterization of derivative **9**)

3.2 Structural characterization of sulfated CAC-like polysaccharides

The postulated sulfation patterns for derivatives **2**, **4-7** and **9** were scrutinized by detailed ¹H- and 2D-NMR analysis. ¹H, ¹³C-DEPT-HSQC spectrum of polysaccharide **2** (Figure 3) clearly showed the presence of ¹H and ¹³C downfield chemical shifted *CH*₂ multiplicity-related signals at $\delta_{\text{H/C}}$ 4.25,4.34/67.8 and 4.17-4.25/69.6 ppm, accounting for *CH*₂ atoms at GlcNAc6S and GalNAc6S 6-position, respectively, as expected from the semi-synthetic strategy to **2** (Scheme 1). The concomitant presence of non-shifted *CH*₂ signals at $\delta_{\text{H/C}}$ 3.65,3.82/61.3 and 3.73,3.90/61.8 ppm indicated that 6-*O*-sulfation proceeded not quantitatively. Degree of sulfation (DS) at primary position of GlcNAc residues could be evaluated by relative integration of methylene signal volumes at $\delta_{\text{H/C}}$ 4.34/67.8 and 3.90/61.8 ppm in the ¹H, ¹³C-DEPT-HSQC spectrum. Since the two signals were associated to the same *CH*₂ atoms in GlcNAc6S and GlcNAc residues, respectively, it could be assumed that they displayed similar ¹*J*_{C,H} coupling constants. However, a difference of around 5–8 Hz from the experimental set value could not cause in any case a substantial variation of the integrated peak volumes (Gargiulo, Lanzetta, Parrilli, & De Castro, 2009; Guerrini, Naggi, Guglieri, Santarsiero, & Torri, 2005). Under this reliable hypothesis, a DS equal to 0.64 was estimated for GlcNAc 6-*O*-sulfation in **2**. As for as GalNAc 6-*O*-sulfation, DS could be not estimated similarly by ¹H, ¹³C-DEPT-HSQC integration, due to signal overlapping. By

looking for alternative signals to be integrated, three different signals were assigned to anomeric α -linked CH atoms of GalNAc units, at $\delta_{H/C}$ 5.61/98.0, 5.54/98.3 and 5.42/98.8, respectively. By comparison with starting LMW HE800 EPS chemical shifts (Supporting Information), the most 1H -upfield shifted signal was easily assigned to unsulfated GalNAc units, while with the aid of a full set (COSY, TOCSY, 1H , ^{13}C -HMBC and 1H , ^{13}C -HSQC-TOCSY) of 2D-NMR spectra it was possible to assign the middle one to GalNAc6S residues. Similarly, the most 1H -downfield shifted signal was associated to α -linked GalNAc units with a different sulfation pattern, in particular with an additional sulfate group at O -3 position as indicated by the marked downfield shift of related CH signal with respect to starting LMW HE800 EPS ($\delta_{H/C}$ 4.51/74.5 vs. 3.88/69.2 ppm, see also Supporting Information). A relative integration of GalNAc, GalNAc6S and GalNAc3,6S anomeric signals in 1H -NMR spectrum of **2** gave DS values equal to 0.65 and 0.16 for 6- O - and 3- O -sulfation, respectively. Finally, the comparison between the 1H , ^{13}C -DEPT-HSQC spectra of **2** and starting LMW HE800 EPS (Supporting Information) clearly showed that signals assigned to GlcA residues in the latter were superimposable to the former one, thus demonstrating that no sulfate groups were present on such units.

Per- O -sulfation of derivative **4** was confirmed by 2D-NMR analysis, giving a single pattern of signals for every monosaccharide constituent of the repeating unit, with a marked 1H and ^{13}C downfield shift of chemical shift values related to every CH and CH_2 atoms at positions not involved in glycosidic linkages or pyranose ring formation (Supporting Information). A comparison of 1H and 1H , ^{13}C -DEPT HSQC spectra of **4** and **5** (Supporting Information) revealed that no significant structural modification of the former happened by MSTFA-mediated desulfation.

2D-NMR spectra analysis of derivative **7** confirmed the postulated structure with a single sulfate group linked to the nitrogen atom of GalN units, as evidenced by the ^{13}C -downfield shift of their CH -2 signal with respect to starting derivative **6** ($\delta_{H/C}$ 3.61/55.8 vs. 3.68/52.4 ppm, see also Supporting Information), in agreement with reported data on N,O -persulfation of chondroitin (Mills et al., 2015). A homogeneous structure for **7** and therefore a quantitative DS for GalNS N -sulfation could be inferred by the single pattern of signals for the whole tetrasaccharide repeating unit (Supporting Information).

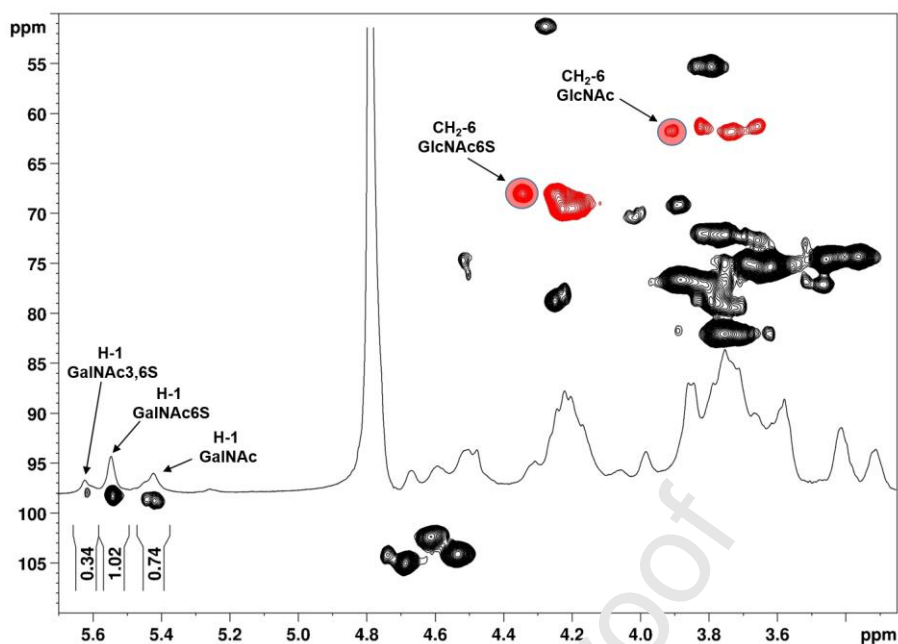


Figure 3: ^1H and $^1\text{H},^{13}\text{C}$ -DEPT-HSQC NMR spectra (200 MHz, 600 MHz, 298 K, D_2O) of **2**

(indicated signals and densities were integrated for estimation of relative amounts of differently sulfated units)

As for polysaccharide **9**, the postulated structure, with GlcNAc 4,6-positions as the only ones not carrying a sulfate group, could not be confirmed by 2D-NMR spectra analysis. Indeed, the only CH_2 multiplicity-edited signals in the $^1\text{H},^{13}\text{C}$ -DEPT-HSQC spectra were found at $^1\text{H}/^{13}\text{C}$ downfield chemical shifted values ($\delta_{\text{H/C}}$ 4.24-4.29/70.0 and 4.20-4.67/68.9 ppm, respectively; see Supporting Information), strongly suggesting that GalNAc and GlcNAc *O*-6 positions were both sulfated. Actually, a comparison of the $^1\text{H},^{13}\text{C}$ -DEPT-HSQC spectra between **9** and per-*O*-sulfated derivative **4** (Supporting Information) revealed a close resemblance, thus suggesting that the multistep strategy relying upon the benzylidene protection of LMW HE800 EPS before treatment with $\text{SO}_3\cdot\text{py}$ in order to avoid per-*O*-sulfation, was not successful. A detailed analysis of a full set (COSY, TOCSY, $^1\text{H},^{13}\text{C}$ -DEPT-HSQC, $^1\text{H},^{13}\text{C}$ -HMBC and $^1\text{H},^{13}\text{C}$ -HSQC-TOCSY) of 2D-NMR spectra of **9** suggested that a significant shortening of the polysaccharide chain happened instead. Indeed, a highly ^1H -downfield and ^{13}C -upfield shifted anomeric signal at $\delta_{\text{H/C}}$ 6.24/93.7 ppm could be detected in the $^1\text{H},^{13}\text{C}$ -DEPT-HSQC spectrum, and assigned by COSY, $^1\text{H},^{13}\text{C}$ -HMBC and $^1\text{H},^{13}\text{C}$ -HSQC-TOCSY correlations to an α -configured 1,4,6-trisulfated GlcNAc pseudo-reducing unit. As confirmation of polysaccharide chain shortening, the densities at $\delta_{\text{H/C}}$ 5.02/76.7 and 5.12/76.1 ppm, detected exclusively in the $^1\text{H},^{13}\text{C}$ -DEPT-HSQC spectrum of **9**, could be assigned to CH -3 and CH -4 atoms, respectively, of a 2,3,4-trisulfated GlcA residue at the non-reducing end of the polysaccharide chain. Noteworthy, signals of different terminally linked residues at both reducing and non-reducing ends could not be found, thus suggesting that the β -1 \rightarrow 4 glycosidic linkage between GlcNAc and GlcA units is much more labile with respect to the other ones constituting the LMW HE800 EPS. Indeed, it is known that the carboxylic

acid moiety can accelerate the hydrolysis of the glycosidic bond involving a 4-linked hexuronic acid by its destabilization through a hydrogen-bond forming a pseudo-pyranosidic ring. By also considering other (stereo)-electronic effects – *e.g.* a hexuronic acid stabilizes its own glycosidic bonds while the acetamido moiety of *N*-acetylated aminosugars can ease the cleavage of the vicinal 1,2-*trans*-configured glycosidic bond by an anchimeric assistance effect (see Figure 4 for details) – the observed selectivity in the acid-catalyzed shortening of LMW HE800 EPS was not surprising at all (Knirel, Naumenko, Senchenkova, & Perepelov, 2019).

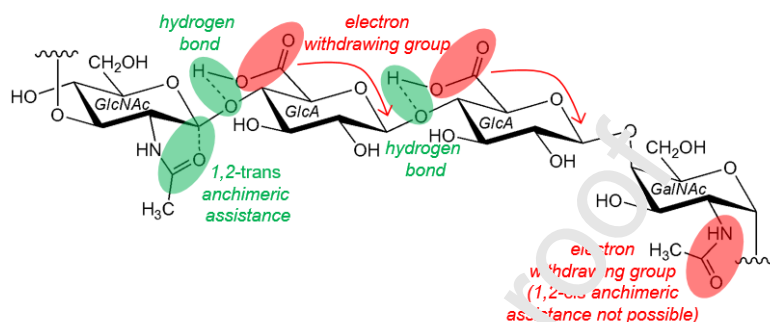


Figure 4: (Stereo)-electronic effects accelerating (green) or decelerating (red) the cleavage of glycosidic bonds in LMW

HE800 EPS repeating unit

	Yield ^{a,b}	DS	M _w ^c [kDa]	M _n ^d [kDa]	M _w /M _n ^e
LMW HE800 EPS	--	0	24.0 ± 0.1	17.6 ± 0.3	1.36 ± 0.02
		GlcNAc 6-sulfation: 0.64			
2	50%	GlcNAc 6-sulfation: 0.65 GalNAc 3-sulfation: 0.16	27.2 ± 0.1	18.8 ± 0.2	1.44 ± 0.02
4	204% (100%)	fully <i>O</i> -sulfated ^f	38.9 ± 0.2	31.8 ± 0.3	1.22 ± 0.04
5	133% (76%)	fully <i>O</i> -sulfated ^f	31.1 ± 0.7	23.1 ± 0.8	1.35 ± 0.06
6	57% (71%)	0	6.2 ± 0.2	3.7 ± 0.2	1.69 ± 0.10
7	53% (49%)	GalNS <i>N</i> -sulfation: 1.00	5.4 ± 0.1	4.2 ± 0.1	1.29 ± 0.05
9	211% (100%)	fully <i>O</i> -sulfated ^f	12.3 ± 0.4	7.5 ± 0.6	1.65 ± 0.14

^a Overall yield calculated from LMW HE800 EPS.

^b For structurally homogeneous polysaccharides, both mass and molar yield could be calculated. The latter is given in parenthesis.

^c Weight averaged molecular mass.

^d Number-averaged molecular mass.

^e Polydispersity index

^f Full *O*-sulfation means that GlcNAc 4,6-sulfation, GalNAc 3,6-sulfation and GlcA 2,3-sulfation degrees are all equal to 2.00

Table 1: Yield and structural data for semi-synthetic polysaccharides **2**, **4-7** and **9**

As further confirmation of the polysaccharide chain shortening in **9** and, more generally, to complete the structural characterization of semi-synthesized LMW HE800 EPS derivatives **2**, **4-7** and **9**, their weight- and number-averaged molecular weights (M_w and M_n, respectively) as well as their polydispersity (as M_w/M_n ratio) were measured by HP-

SEC-MALLS analysis. A significant chain shortening with respect to starting LMW HE800 EPS was detected for derivatives **6**, **7** and **9**, even if no dramatic increase of polydispersity index was noted (Table 1).

3.3 Binding affinity of sulfated GAG-like polysaccharides with growth factors

The GAG-mimetic potential of the HE800 derivatives, and in particular, the impact of the well-defined sulfate positions on the growth factor binding affinity was assessed by Surface Plasmon Resonance (SPR). GAGs are known to bind various signaling proteins, such as growth factors, and are thus involved in both physiological and pathological processes, including organogenesis, wound healing, coagulation, inflammation, thrombosis, cancer growth and metastasis (Köwitsch, Zhou, & Groth, 2018). By interacting with growth factors, GAGs protect them from undesired degradation and enhance both their local concentration up to levels required for signaling and their stability, thus facilitating the growth factor binding to their cell receptors (Gandhi & Mancera, 2008). Five basic growth factors, namely TGF- β 1, BMP-2, VEGF, GDF-5 and FGF-2, and one acidic growth factor, EGF, were tested (Table 2). Starting LMW HE800 EPS, although devoid of sulfate groups, displayed similar binding affinity to basic growth factors as heparin. In the case of sulfated GAGs, such as heparin, the main contribution to binding affinity comes from electrostatic interactions between negatively charged sulfate groups of GAGs and clusters of positively charged, basic amino acids (such as arginine, lysine and histidine) on growth factors, that constitute the so-called “heparin-binding domains” (Gandhi & Mancera, 2008). Other non-covalent interactions, such as hydrogen bonding between polar amino acids and polysaccharide hydroxyl groups may also contribute to the polysaccharide/growth factor binding. In the HE800 structure, the presence in the repeating unit of two consecutive uronic acids, carrying negatively charged carboxylate moieties together with free hydroxyls, may promote the polysaccharide/growth factor interactions. In contrast, unsulfated derivative **6** exhibited no growth factor binding ability, which can result from its considerably lower molecular weight compared to LMW HE800 EPS, presumably not sufficient to establish efficient binding. A chemoselective sulfation of the single free amine on GalNAc unit, leading to derivative **7**, led to only a slight increase in growth factor binding. Similarly, when sulfate groups were placed almost exclusively at *O*-6 positions of GlcNAc and GalNAc units (derivative **2**), no binding enhancement was further observed. However, in the case of the derivative **4**, having the tetrasaccharide repeating unit fully *O*-sulfated, a clear increase in the growth factor binding was measured. Interestingly, this affinity was considerably higher for the derivative **9**, that is fully *O*-sulfated as well and displays a significantly lower M_w with respect to derivative **4**. Basic growth factors displayed higher affinity for both highly sulfated derivatives **4** and **9**, comparing to heparin. No binding affinity was measured between the acidic Epidermal Growth Factor (EGF) and all the LMW HE800 EPS derivatives and heparin, thus emphasizing the electrostatic origin of the interactions between the LMW HE800 EPS derivatives and basic growth factors. It could be concluded that GAG-

mimetic potential of LMW HE800 EPS and its derivatives results from both sulfate and carboxylic groups, which are determinant for the growth factor binding to the polysaccharide chains. The polysaccharide molecular weight also highly impacts the association with proteins, as a decrease in molecular weight significantly increased the binding affinity for the same sulfation pattern (derivatives **4** and **9**). However, only *in vitro* and *in vivo* studies could evidence the most efficient sulfation pattern able to induce specific biological activities.

	TGF-β1	BMP-2	VEGF	GDF-5	FGF-2	EGF
LMW HE800 EPS	$9.1 \cdot 10^{-8}$	$3.5 \cdot 10^{-8}$	$1.7 \cdot 10^{-8}$	$5.8 \cdot 10^{-8}$	$4.0 \cdot 10^{-8}$	$>10^{-5}$
2	$5.2 \cdot 10^{-7}$	$5.0 \cdot 10^{-7}$	$2.2 \cdot 10^{-7}$	$1.2 \cdot 10^{-7}$	$4.1 \cdot 10^{-7}$	$>10^{-5}$
4	$2.2 \cdot 10^{-9}$	$7.6 \cdot 10^{-9}$	$1.3 \cdot 10^{-8}$	$1.4 \cdot 10^{-9}$	$5.9 \cdot 10^{-9}$	$>10^{-5}$
6	$>10^{-5}$	$>10^{-5}$	$>10^{-5}$	$9.4 \cdot 10^{-7}$	$>10^{-5}$	$>10^{-5}$
7	$>10^{-5}$	$3.1 \cdot 10^{-6}$	$1.8 \cdot 10^{-5}$	$2.1 \cdot 10^{-7}$	$2.9 \cdot 10^{-6}$	$>10^{-5}$
9	$4.8 \cdot 10^{-10}$	$6.2 \cdot 10^{-10}$	$7.7 \cdot 10^{-10}$	$0.6 \cdot 10^{-10}$	$2.6 \cdot 10^{-9}$	$>10^{-5}$
heparin	$1.9 \cdot 10^{-8}$	$8.3 \cdot 10^{-9}$	n.d. ^a	$6.5 \cdot 10^{-8}$	$1.0 \cdot 10^{-8}$	$>10^{-5}$

^a Not determined

Table 2: Dissociation constant (K_d [M]) values for the interaction of LMW HE800 EPS derivatives and heparin with growth factors.

4. Conclusions

Four different semi-synthetic strategies were proposed for the structural modification of LMW EPS from the marine bacterium *V. diabolicus* HE800 strain, in order to obtain new, regioselectively sulfated polysaccharides acting as GAG-mimics. A detailed structural characterization through 2D-NMR and HP-SEC-MALLS analysis revealed that, among the six obtained, semi-synthetic polysaccharides, three different sulfation patterns (per-*O*-sulfation, a single *N*-sulfation and a selective primary hydroxyl sulfation) were achieved, with molecular weights ranging from 5 to 40 kDa. A SPR investigation of the affinity between a set of such polysaccharides (LMW HE800 EPS and five of the obtained derivatives thereof) and a set of six growth factors revealed, as expected, that binding strength is primarily depending on polysaccharide sulfation degree. In particular, a much stronger binding was detected for per-*O*-sulfated derivatives with respect to the rest of polysaccharides showing an overall DS (defined as the the average number of sulfate groups per polysaccharide repeating unit) ranging from 0 to 1.5. Since oversulfated GAG polysaccharides can induce strong allergic-type responses in humans causing severe adverse events, an investigation of the growth factor affinity profile of LMW HE800 EPS derivatives with overall DS values spanning between 1.5 and 8 (the latter being the value for a per-*O*-sulfated derivative) should be planned. Such new semi-synthetic targets may have a well-defined sulfation pattern too, in order to assess any eventual effect of sulfate groups distribution on the affinity with growth factors. To this aim, new semi-synthetic strategies from LMW HE800 EPS are currently under investigation employing suitable sequences

of tailored chemical steps for GAG sulfation pattern modification. If they will be successful, SPR studies with growth factors will be done and results reported elsewhere.

CRedit authorship contribution statement

Fabiana Esposito: Data curation, Investigation, Writing - review & editing. **Giulia Vessella:** Data curation, Investigation, Writing - review & editing. **Corinne Sinquin:** Data curation, Investigation. **Serena Traboni:** Conceptualization, Writing - review & editing. **Alfonso Iadonisi:** Conceptualization, Writing - review & editing. **Sylvia Collic-Jouault:** Conceptualization, Writing - review & editing. **Agata Zykwińska:** Investigation, Validation, Conceptualization, Writing - review & editing. **Emiliano Bedini:** Conceptualization, Funding acquisition, Methodology, Validation, Writing – original draft.

Declaration of Competing Interest

The authors report no declarations of interest.

Acknowledgments

The authors would like to thank Mike Maillasse for SPR measurements (Impact Platform, Nantes). This research was funded by University of Naples Federico II (TPA 2020-B grant).

References

- Arlov, Ø., Rüttsche, D., Koraven, M., Öztürk, E., & Zenobi-Wong, M. (2021) Engineered sulfated polysaccharides for biomedical applications. *Advanced Functional Materials*, 2010732. doi.org/10.1002/adfm.202010732
- Bachelder, E. M., Pino, E. N., & Ainslie, K. M. (2017) Acetalated dextran: A tunable and acid-labile biopolymer with facile synthesis and a range of applications. *Chemical Reviews*, 117, 1915–1926. doi.org/10.1021/acs.chemrev.6b00532
- Badri, A., Williams, A., Linhardt, R.J. & Koffas, M.A.G. (2018) The road to animal-free glycosaminoglycan production: current efforts and bottlenecks. *Current Opinion in Biotechnology*, 53, 85–92. doi.org/10.1016/j.copbio.2017.12.018
- Badri, A., Williams, A., Awofiranye, A., Datta, P., Xia, K., He, W., Fraser, K., Dordick, J.S., Linhardt, R.J., & Koffas, M.A.G. (2021) Complete biosynthesis of a sulfated chondroitin in *Escherichia coli*. *Nature Communications*, 12, 1389. doi.org/10.1038/s41467-021-21692-5

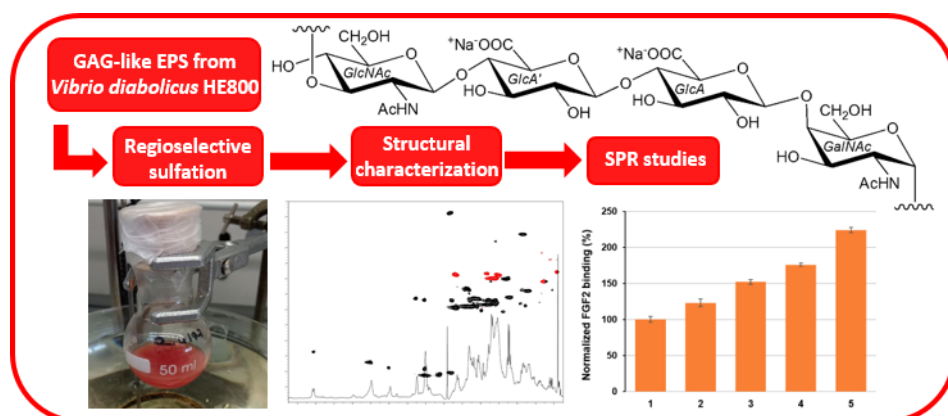
- Bedini, E., De Castro, C., De Rosa, M., Di Nola, A., Iadonisi, A., Restaino, O. F., Schiraldi, C., & Parrilli, M. (2011). A microbiological-chemical strategy to produce chondroitin sulfate A,C. *Angewandte Chemie International Edition*, *50*, 6160–6163. [dx.doi.org/10.1002/anie.201101142](https://doi.org/10.1002/anie.201101142)
- Bedini, E., Laezza, A., & Iadonisi, A. (2016) Chemical derivatization of sulfated glycosaminoglycans. *European Journal of Organic Chemistry*, 3018–3042. doi.org/10.1002/ejoc.201600108
- Bedini, E., Laezza, A., Parrilli, M., & Iadonisi, A. (2017) A review of chemical methods for the selective sulfation and desulfation of polysaccharides *Carbohydrate Polymers*, *174*, 1224–1239. [dx.doi.org/10.1016/j.carbpol.2017.07.017](https://doi.org/10.1016/j.carbpol.2017.07.017)
- Bedini, E., Corsaro, M.M., Fernández-Mayoralas, A., & Iadonisi, A. (2019) Chondroitin, dermatan, heparan, and keratan sulfate: structure and functions. In: Cohen, E. & Merzendorfer, H. (Eds), *Extracellular sugar-based biopolymers matrices* (pp. 187–233). Berlin: Springer. doi.org/10.1007/978-3-030-12919-4_5
- Casillo, A., Lanzetta, R., Parrilli, M., & Corsaro, M.M. (2018) Exopolysaccharides from marine and marine extremophilic bacteria: structures, properties, ecological roles and applications. *Marine Drugs*, *16*, 69. doi.org/10.3390/md16020069
- Chien, C.-Y., Enomoto, Y., & Iwata, T. (2019). Synthesis of C2-regioselectively substituted curdlan acetate propionate and the effect of C2 substituent on their properties. *ACS Sustainable Chemistry & Engineering*, *7*, 9857–9864. doi.org/10.1021/acssuschemeng.9b00415
- Collin, E.C, Carroll, O., Kilcoyne, M., Peroglio, M., See, E., Hendig, D., Alini, M., Grad, S., & Pandit, A. (2017). Ageing affects chondroitin sulfates and their synthetic enzymes in the intervertebral disc. *Signal Transduction and Targeted Therapy*, *2*, 17049. doi.org/10.1038/sigtrans.2017.49
- DeAngelis, P.L. (2012). Glycosaminoglycan polysaccharide biosynthesis and production: today and tomorrow. *Applied Microbiology and Biotechnology*, *94*, 295–305. doi.org/10.1007/s00253-011-3801-6.
- Delbarre-Ladrat, C., Siquin, C., Lebellenger, L., Zykwinska, A., & Collic-Jouault, S. (2014) Exopolysaccharides produced by marine bacteria and their applications as glycosaminoglycan-like molecules. *Frontiers in Chemistry*, *2*, 85. doi.org/10.3389/fchem.2014.00085
- Gandhi, N.S. & Mancera, R.L. (2008) The structure of glycosaminoglycans and their interactions with proteins. *Chemical Biology and Drug Design*, *72*, 455–482. doi.org/10.1111/j.1747-0285.2008.00741.x
- Gargiulo, V., Lanzetta, R., Parrilli, M., & De Castro, C. (2009) Structural analysis of chondroitin sulfate from *Scyliorhinus canicula*: a useful source of this polysaccharide. *Glycobiology*, *19*, 1485–1491. doi.org/10.1093/glycob/cwp123
- Gomez D’Ayala, G., Malinconico, M., & Laurienzo, P. (2008) Marine derived polysaccharides for biomedical applications: chemical modification approaches. *Molecules*, *13*, 2069–2106. doi.org/10.3390/molecules13092069

- Guerrini, M., Naggi, A., Guglieri, S., Santarsiero, R., & Torri, G. (2005) Complex glycosaminoglycans: profiling substitution patterns by two-dimensional nuclear magnetic resonance spectroscopy. *Analytical Biochemistry*, *337*, 35–47. doi.org/10.1016/j.ab.2004.10.012
- Guo, Y., & Conrad, H.E. (1989) The disaccharide composition of heparins and heparan sulfates. *Analytical Biochemistry*, *176*, 96–104. doi.org/10.1016/0003-2697(89)90278-9
- Han, X., Sanderson, P., Nesheiwat, S.; Lin, L., Yu, Y., Zhang, F., Amster, I.J., & Linhardt, R.J. (2020) Structural analysis of urinary glycosaminoglycans from healthy human subjects. *Glycobiology*, *30*, 143–151. doi.org/10.1093/glycob/cwz088
- Hardingham, T. (1995) Changes in chondroitin sulphate structure induced by joint disease. *Acta Orthopaedica Scandinavica*, *66*, 107–110. doi.org/10.3109/17453679509157663
- Jin, X., Zhang, W., Wang, Y., Sheng, J., Xu, R., Li, J., Du, G., & Kang Z. (2021) Biosynthesis of non-animal chondroitin sulfate from methanol using genetically engineered *Pichia pastoris*. *Green Chemistry*, *23*, 4365–4374. doi.org/10.1039/d1gc00260k
- Kamerling, J.P., Gerwing, G.J., Vliegthart, J.F., & Camp, J. R. (1975) Characterization by gas-liquid chromatography-mass spectrometry and proton-magnetic resonance spectroscopy of pertrimethylsilyl methyl glycosides obtained in the methanolysis of glycoproteins and glycopeptides. *Biochemical Journal*, *151*, 491–495. https://doi.org/10.1042/bj1510491
- Knirel, Y.A., Naumenko, O.I., Senchenkov, S.N., & Perepelov, A.V. (2019) Chemical methods for selective cleavage of glycosidic bonds in the structural analysis of bacterial polysaccharides. *Russian Chemical Reviews*, *88*, 406–424. doi.org/10.1070/RCR4856
- Köwitsch, A., Zhou, G., & Grottel T. (2018) Medical application of glycosaminoglycans: A review. *Journal of Tissue Engineering and Regenerative Medicine*, *12*, e23–e41. doi.org/10.1002/term.2398
- Laezza, A., De Castro, C., Parrilli, M., & Bedini, E. (2014). Inter vs. intraglycosidic acetal linkages control sulfation pattern in semi-synthetic chondroitin sulfate. *Carbohydrate Polymers*, *112*, 546–555. dx.doi.org/10.1016/j.carbpol.2014.05.085
- Li, G., Cai, C., Li, L., Fu, L., Chang, Y., Zhang, F., Toida, T., Xue, C., & Linhardt, R.J. (2014) Method to detect contaminants in heparin using radical depolymerization and liquid chromatography–mass spectrometry. *Analytical Chemistry*, *86*, 326–330. doi.org/10.1021/ac403625a
- Lin, L., Li, S., Gao, N., Wang, W., Zhang, T., Yang, L., Yang, X., Luo, D., Ji, X., & Zhao, J. (2021) The toxicology of native fucosylated glycosaminoglycans and the safety of their depolymerized products as anticoagulants. *Marine Drugs*, *19*, 487. doi.org/10.3390/md19090487

- Lindahl, U., Li, J., Kusche-Gellberg, M., Salmivirta, M., Alaranta, S., Veromaa, T., Emeis, J., Roberts, I. Taylor, C., Oreste, P. et al. (2005) Generation of “neoheparin” from *E. coli* K5 capsular polysaccharide. *Journal of Medicinal Chemistry*, 48, 349–352. doi.org/10.1021/jm049812m
- Mans, D.J., Ye, H., Dunn, J.D., Kolinski, R.E., Long, D.S., Phatak, N.L., Ghasriani, H., Buhse, L.F., Kauffman, J.F., & Keire, D.A. (2015) Synthesis and detection of *N*-sulfonated oversulfated chondroitin sulfate in marketplace heparin. *Analytical Biochemistry*, 490, 52–54. doi.org/10.1016/j.ab.2015.08.003
- Mende, M., Bednarek, C., Wawrzyszyn, M., Sauter, P., Biskup, M. B., Schepers, U., & Bräse, S. (2016). Chemical synthesis of glycosaminoglycans. *Chemical Reviews*, 116, 8193–8255. doi.org/10.1021/acs.chemrev.6b00010
- Montreuil, J., Bouquelet, S., Debray, H., Fournet, B., Spik, G., & Strecker, G. (1986) Glycoproteins. In Chaplin, M.F. & Kennedy, J.F. (Eds), *Carbohydrate analysis. A practical approach* (pp. 143–204). Oxford: IRL Press.
- Nadkarni, V.D., Toida, T., Van Gorp, C.L., Schubert, R.L., Weiler, J.M., Hansen, K.P., Caldwell, E.E.O., & Linhardt, R.J. (1996) Preparation and biological activity of *N*-sulfonated chondroitin and dermatan sulfate derivatives. *Carbohydrate Research*, 290, 87–96. doi.org/10.1016/0008-6215(96)00129-2
- Palhares, L.C.G.F., London, J.A., Kozłowski, A.M., Espoito, E., Chavante, S.F., Ni, M., & Yates, E.A. (2021) Chemical modification of glycosaminoglycan polysaccharides. *Molecules*, 26, 5211. doi.org/10.3390/molecules26175211
- Raguénès, G., Christen, R., Guezennec, J., Pignet, P., & Barbier, G. (1997). *Vibrio diabolicus* sp. nov., a new polysaccharide-secreting organism isolated from a deep-sea hydrothermal vent polychaete annelid, *Alvinella pompejana*. *International Journal of Systematic and Evolutionary Microbiology*, 47, 989–995. doi.org/10.1099/00207713-47-4-989
- Restaino, O.F., Finamore, R., Stellavaco, A., Diana, P., Bedini, E., Trifuoggi, M., De Rosa, M., & Schiraldi, C. (2019) European chondroitin sulfate and glucosamine food supplements: a systematic quality and quantity assessment compared to pharmaceuticals. *Carbohydrate Polymers*, 222, 114984. doi.org/10.1016/j.carbpol.2019.114984
- Rougeaux, H., Kervarec, N., Pichon, R., & Guezennec, J. (1999) Structure of the exopolysaccharide of *Vibrio diabolicus* isolated from a deep-sea hydrothermal vent. *Carbohydrate Research*, 322, 40–45. doi.org/10.1016/S0008-6215(99)00214-1
- Sakamoto, J., Kita, R., Duelamae, I., Kunitake, M., Hirano, M., Yoshihara, D., Yamamoto, T., Noguchi, T., Roy, B., & Shinkai, S. (2017). Cohelical crossover network by supramolecular polymerization of a 4,6-acetalized β -1,3-glucan macromer. *ACS Macro Letters*, 6, 21–26. doi.org/10.1021/acsmacrolett.6b00706
- Senni, K., Gueniche, F., Changotade, S., Septier, D., Sinquin, C., Ratiskol, J., Lutomski, D., Godeau, G., Guezennec, J., & Collic-Jouault, S. (2013) Unusual glycosaminoglycans from a deep sea hydrothermal bacterium improve fibrillar

- collagen structuring and fibroblast activities in engineered connective tissues. *Marine Drugs*, *11*, 1351–1369. doi.org/10.3390/md11041351
- Soares da Costa, D., Reis, R.L., & Pashkuleva, I. (2017) Sulfation of glycosaminoglycans and its implications in human health and disorders. *Annual Review of Biomedical Engineering*, *19*, 1–26. doi.org/ 10.1146/annurev-bioeng-071516-044610
- Takano, R., Kanda, T., Hayashi, K., Yoshida, K., & Hara, S. (1995). Desulfation of sulfated carbohydrates mediated by silylating reagents. *Journal of Carbohydrate Chemistry*, *14*, 885–888. doi.org/10.1080/07328309508005382
- Valoti, E., Miraglia, N., Bianchi, D., Valetti, M., & Bazza, P. (2012). Shark-like chondroitin sulphate and process for the preparation thereof. *US Patent*, 8664196B2.
- Vessella, G., Traboni, S., Cimini, D., Iadonisi, A., Schiraldi, C., & Bedini, E. (2019) Development of semisynthetic, regioselective pathways for accessing the missing sulfation patterns of chondroitin sulfate. *Biomacromolecules*, *20*, 3021–3030. doi.org/10.1021/acs.biomac.9b00590
- Vessella, G., Esposito, F., Traboni, S., Di Meo, C., Iadonisi, A., Schiraldi, C., & Bedini, E. (2021) Exploiting diol reactivity for the access to unprecedented low molecular weight curdlan sulfate polysaccharides. *Carbohydrate Polymers*, *269*, 118324. doi.org/10.1016/j.carbpol.2021.118324
- Yan, L., Li, J., Wang, D., Ding, T., Hu, Y., Ye, X., Linhardt, R.J. & Chen, S. (2017) Molecular size is important for the safety and selective inhibition of intrinsic factor Vase for fucosylated chondroitin sulfate. *Carbohydrate Polymers*, *178*, 180–189. 10.1016/j.carbpol.2017.09.034
- Zanchetta, P., Lagarde, N., & Guezenec, J. (2003) A new bone-healing material: a hyaluronic acid-like bacterial exopolysaccharide. *Calcified Tissue International*, *72*, 74–79. doi.org/10.1007/s00223-001-2091-x
- Zeng, K., Groth, T., & Zhang, K. (2018) Recent advances in artificially sulfated polysaccharides for applications in cell growth and differentiation, drug delivery, and tissue engineering. *ChemBioChem*, *20*, 737–746. doi.org/10.1002/cbic.201800569
- Zhang, X., Lin, L., Huang, H., & Linhardt, R.J. (2020) Chemoenzymatic synthesis of glycosaminoglycans. *Accounts of Chemical Research*, *53*, 335–346. doi.org/10.1021/acs.accounts.9b00420
- Zhao, L., Lai, S., Huang, R., Wu, M., Gao, N., Xu, L., Qin, H., Peng, W., & Zhao, J. (2013) Structure and anticoagulant activity of fucosylated glycosaminoglycan degraded by deaminative cleavage. *Carbohydrate Polymers*, *98*, 1514–1523. doi.org/10.1016/j.carbpol.2013.07.063

Graphical abstract



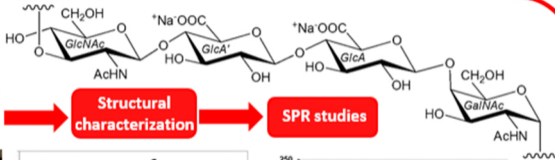
Declaration of interests

The authors declare that they have no known competing financial interests or personal relationships that could have appeared to influence the work reported in this paper.

The authors declare the following financial interests/personal relationships which may be considered as potential competing interests:

Journal Pre-proof

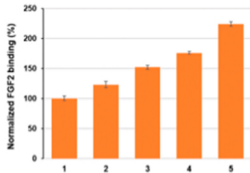
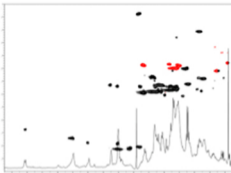
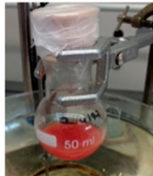
**GAG-like EPS from
Vibrio diabolicus HE800**



**Regioselective
sulfation**

**Structural
characterization**

SPR studies



Graphics Abstract

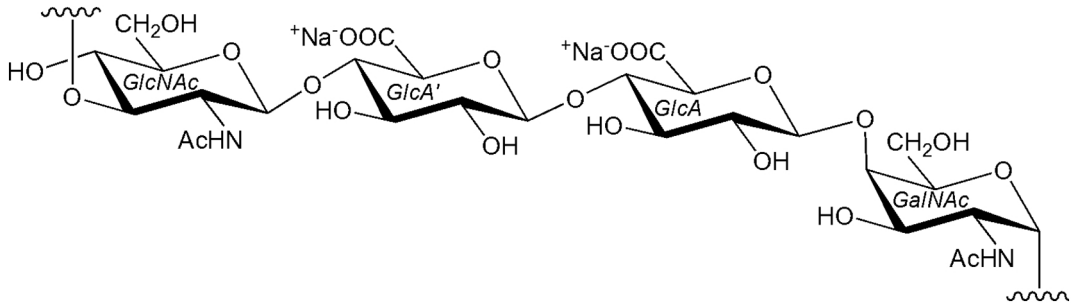


Figure 1

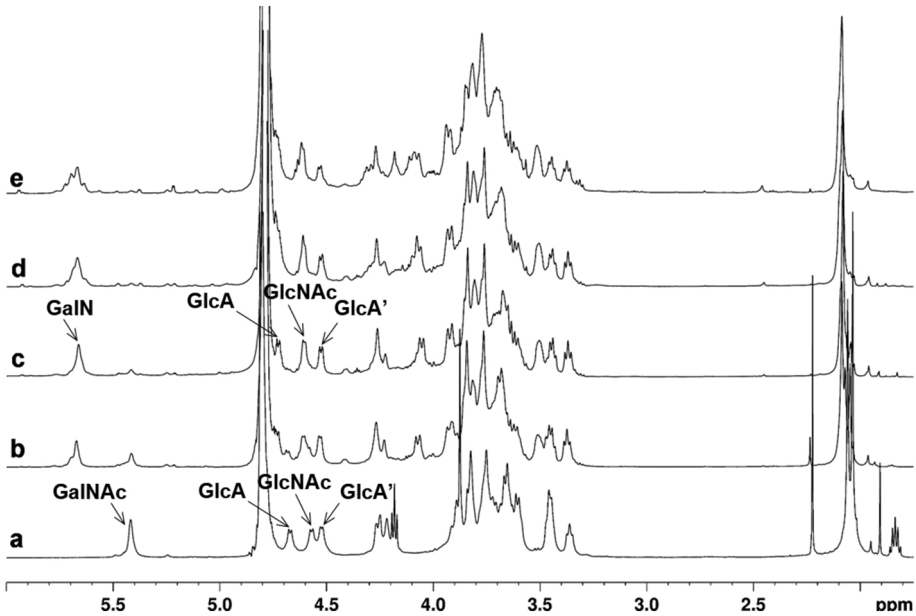


Figure 2

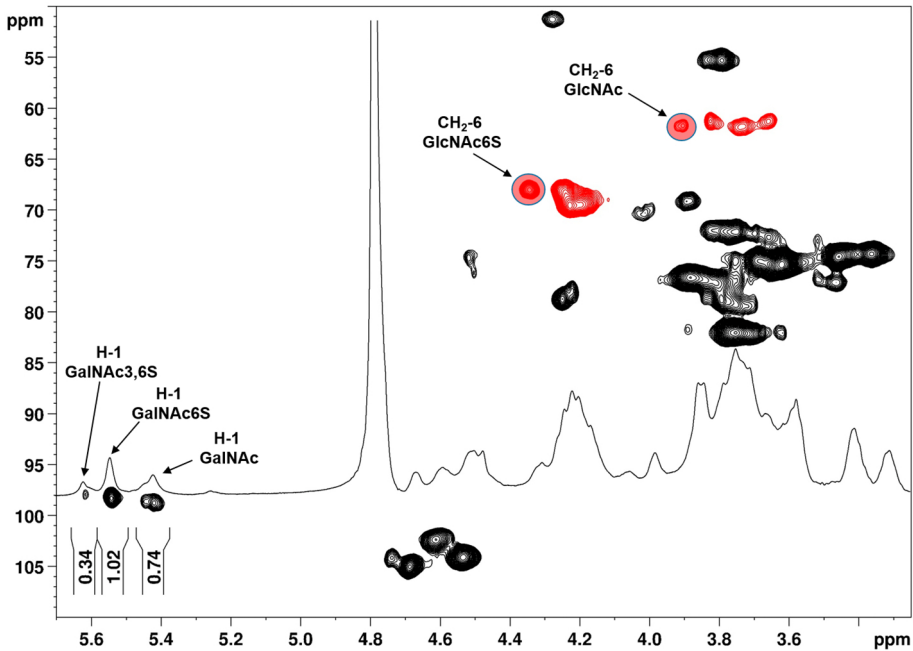


Figure 3

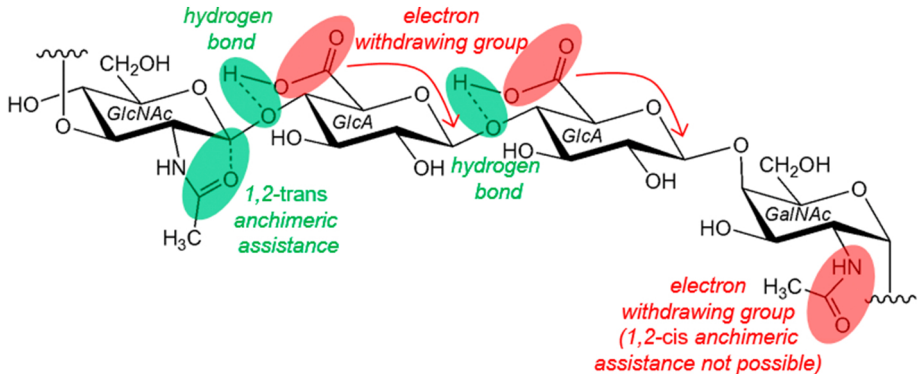


Figure 4